Spectrochimica Acta Part A: Molecular and Biomolecular Spectroscopy 226 (2020) 117571

Contents lists available at ScienceDirect

Spectrochimica Acta Part A: Molecular and Biomolecular Spectroscopy

journal homepage: www.elsevier.com/locate/saa

Aggregation induced emission-active two-photon absorption zwitterionic chromophore for bioimaging application

Fei Meng [a, b, 1], Chengkai Zhang [a, 1], Dandan Li [a, *], Yupeng Tian [a, **]

[a] Institute of Physics Science and Information Technology, College of Chemistry and Chemical Engineering, Key Laboratory of Functional Inorganic Materials Chemistry of Anhui Province, Anhui Province Key Laboratory of Chemistry for Inorganic/Organic Hybrid Functionalized Materials, Key Laboratory of Structure and Functional Regulation of Hybrid Materials of Ministry of Education, Anhui University, Hefei, 230601, PR China
[b] Department of Food and Environmental Engineering, Chuzhou Vocational and Technical College, Chuzhou, 239000, PR China

ARTICLE INFO

Article history:
Received 15 August 2019
Received in revised form
18 September 2019
Accepted 27 September 2019
Available online 10 October 2019

Keywords:
Two-photon
Aggregation induced emission
Mitochondria
Bioimaging

ABSTRACT

The fabrication of two-photon absorption material is a versatile approach to achieve high resolution bioimaging with low phototoxicity yet remain sophisticated. Herein, a zwitterionic chromophore, **MF**, with D-π-A configuration has been rational designed and synthesized. Remarkably, **MF** exhibited enhanced one- and two-photon fluorescent in the aggregation states. Additionally, the obtained **MF NPs** encapsulated by Pluronic F-127, could be employed as a two-photon fluorescent probe for bioimaging. The results reveal that **MF NPs** could target mitochondria by using two-photon confocal microscopy and stimulated emission depletion nanoscopy methods.

© 2019 Elsevier B.V. All rights reserved.

1. Introduction

As the powerhouses of the cell, mitochondria are highly dynamic organelles regulated by coordinated fission and fusion events [1]. Previous works have revealed that damaged or unwanted mitochondria can be selectively cleared away during the mitophagy process to maintain a healthy population of mitochondria [2–5]. Furthermore, amounts of studies unveiled that mitochondrial dynamics play crucial roles in controlling antitumor immune responses [6]. In this sense, visualizing mitochondrial dynamic changes is vital important in the fields of physiology, pathology and pharmacology.

Thanks to its remarkable sensitivity, excellent spatial resolution and noninvasive operation, fluorescence microscopy has become a powerful tool for medical and biological applications [7–16]. Thereinto, benefit from the near infrared excitation light, two-photon confocal microscopy has been exploited as an optimized approach for bioimaging with deeper tissue penetration, higher spacial resolution and weaker specimen photodamage [17–24]. Therefore, the search for novel two-photon absorbing materials with optimized biocompatibility has been found to be a critical determination for bioimaging, and which exhibit excellent fluorescence under physiological condition is a highly desired target.

Bearing these considerations in mind, herein, we deployed a systematic protocol to fabricate an ionic character or a complete charge separation (i.e., zwitterionic) 2 PA chromophore within a D-π-A model, **MF** (Scheme 1). The results show that **MF** displays enhanced charge mobility and unveils obviously two-photon activity in near infrared region because of its zwitterionic feature [25,26]. In addition, the cationic properties drive it into mitochondria *via* electrostatic interaction [27] to visualize mitochondrial dynamic changes under two-photon confocal microscopy and stimulated emission depletion nanoscopy methods.

2. Experiments

The synthetic routes of intermediate materials and target molecular (**MF**) in this work were shown in supporting information (Scheme S1). As for **MF**, the synthetic procedure and characterization data was displayed as follows: **M2** (1 g, 3 mmol) was dissolved in ethyl alcohol completely, then **F1** (1.26 g, 5 mmol) was added successively. The reaction was stirred at 80 °C for 5 h. The mixture was cooled to room temperature. Filtration with red product, yield 81.9%. ^{1}H NMR (400 MHz, DMSO-d_6) δ 9.11 (s, 1H), 8.73 (d, J = 16.1 Hz, 1H), 8.45 (d, J = 8.6 Hz, 1H), 8.38 (d, J = 8.6 Hz, 1H), 8.33

* Corresponding author.
** Corresponding author.
E-mail addresses: chemlidd@163.com (D. Li), yptian@ahu.edu.cn (Y. Tian).
[1] These authors contributed equally to this work.

https://doi.org/10.1016/j.saa.2019.117571
1386-1425/© 2019 Elsevier B.V. All rights reserved.

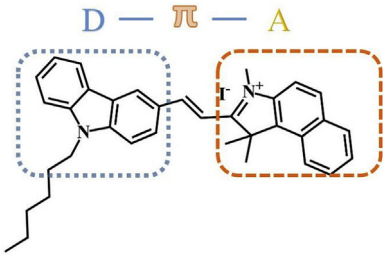

Scheme 1. Structure of **MF**.

(m, 2H), 8.22 (d, $J = 8.1$ Hz, 1H), 8.10 (s, 1H), 7.83 (dd, $J = 20.5$, 8.7 Hz, 2H), 7.78 (m, 3H), 7.58 (t, $J = 7.6$ Hz, 1H), 7.37 (t, $J = 7.2$ Hz, 1H), 4.51 (s, 2H), 4.28 (s, 2H), 2.07 (s, 6H), 1.99 (s, 2H), 1.86 (d, $J = 36.2$ Hz, 3H), 1.23 (s, 6H), 0.82 (d, $J = 6.9$ Hz, 3H). ^{13}C NMR (100 MHz, DMSO-d_6) δ (ppm): 205.18, 154.91, 143.88, 141.56, 137.64, 133.68, 131.06, 130.36, 128.90, 128.25, 128.23, 127.36, 126.88, 125.85, 125.06, 121.39, 112.68, 110.18, 110.07, 108.81, 53.79, 42.99, 35.00, 31.41, 28.87, 26.45, 25.53, 22.26, 13.27. ESI-MS: calculated for $[M]^+$: 485.3, *found* 485.3.

3. Results and discussion

Several techniques have been adopted to investigate the optical properties of the target molecule **MF**. Firstly, we set out to investigate the linear optical photophysical properties (absorption and emission spectra in different solvents) of **MF** (Fig. 1). As shown in Fig. 1a, **MF** features one intense absorption band (about 500 nm), which originates from the $\pi-\pi^*$ or intramolecular charge transfer (ICT) transition. With the aid of time-dependent density functional theory (TD-DFT) calculations (Fig. S1), the obviously ICT can be found within **MF** molecule. Interestingly, the solvability variation of **MF** in different solutions lead to obviously difference of fluorescent intensity (Fig. 1b). It motivated us to study its emission behavior in aggregation state in detail.

As displayed in Fig. 2a, the emission spectra of **MF** in water/ethanol mixtures with different ethanol fractions (*fe*, the volume percentage of ethanol in water mixtures) were collected. The result unambiguously reflect that the fluorescence intensity of **MF** increased with increasing *fe* and accompanied with a small red-shift emission, revealing the aggregation induced emission (AIE) activity of **MF**. Considering the structure feature of **MF**, the above phenomenon can be ascribed to the fact that the restriction of intramolecular rotations (RIR) of the methyne within **MF** in the aggregation state could enhance light emission [24]. Notably, AIE-active molecule **MF** can effectively avoid the unwanted aggregation-caused quenching due to the s high tendency of self-aggregate under physiological conditions [28,29].

Encouraged by the above results, the AIE-active nanoparticles (NPs) of **MF** for biological experiments were prepared via a reported nano-precipitation method using Pluronic F-127 (F127) as the matrix in our recent work [30]. For size distribution analysis, **MF NPs** revealed an average size of 30 ± 30 nm (Fig. 2b) evaluating

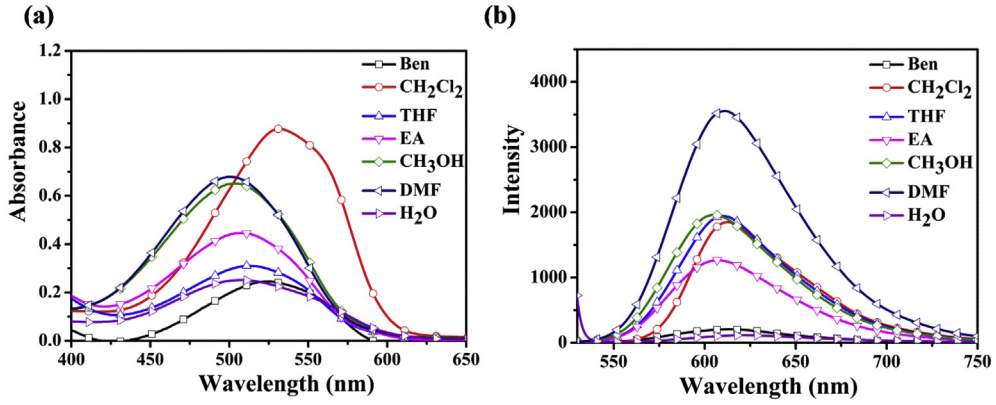

Fig. 1. UV-*vis* absorption spectra (a) and one photon fluorescence spectra (b) of **MF** in different solvents (c = 10^{-5} M).

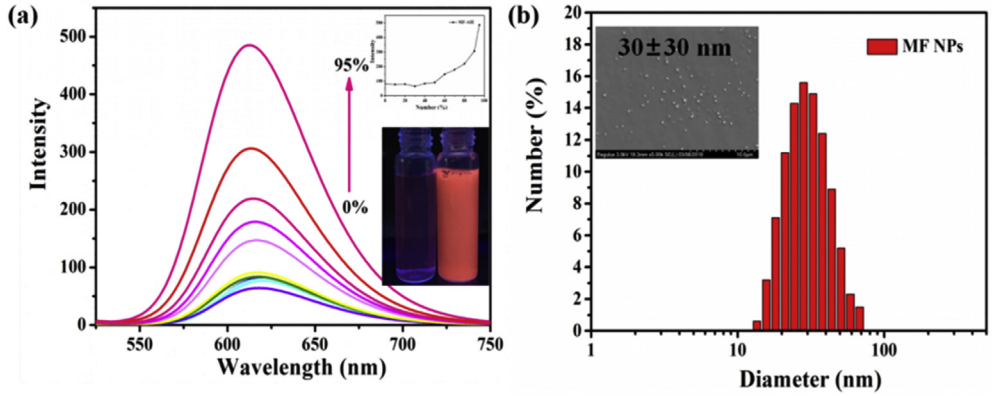

Fig. 2. (a) Fluorescence spectra changes of **MF** in water with different ethanol fractions. (b) DLS of **MF** in water/ethanol (10/90, v/v) and SEM images (inset) of **MF** in ethanol fraction 90%.

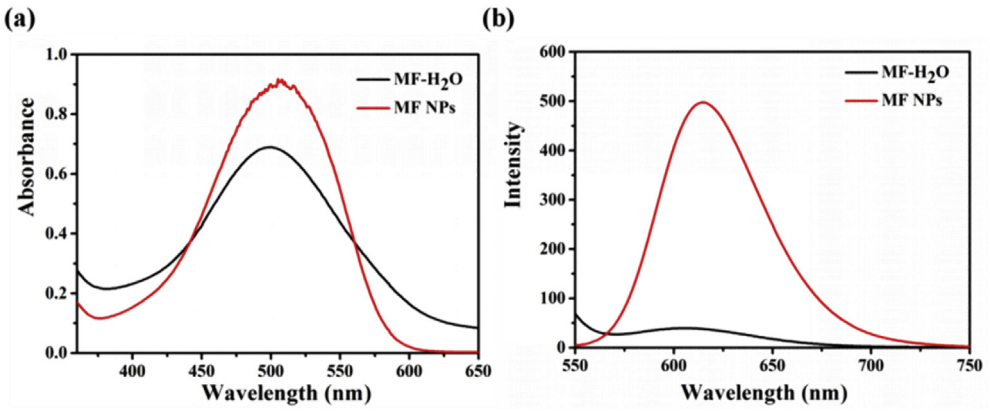

Fig. 3. UV-*vis* absorption spectra (a) and one-photon fluorescence emission spectra (b) of in water and aggregation state.

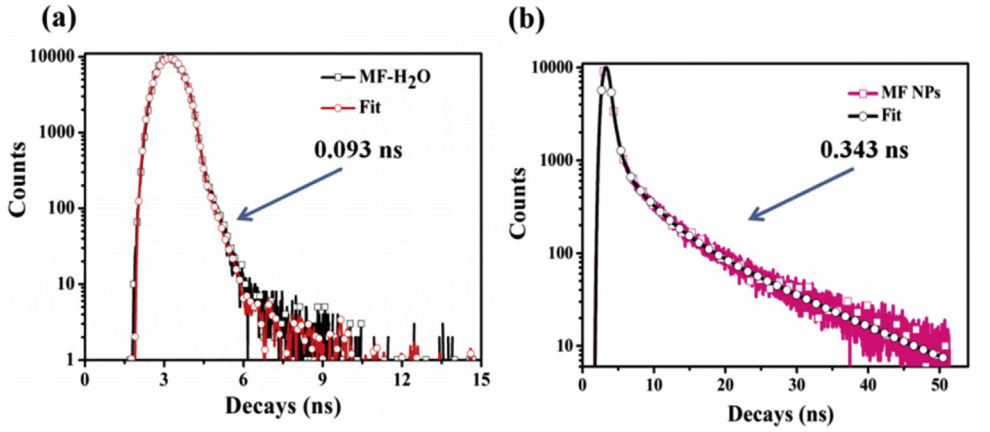

Fig. 4. Time-resolved fluorescent spectra of **MF-H_2O** (a) and **MF NPs** (b).

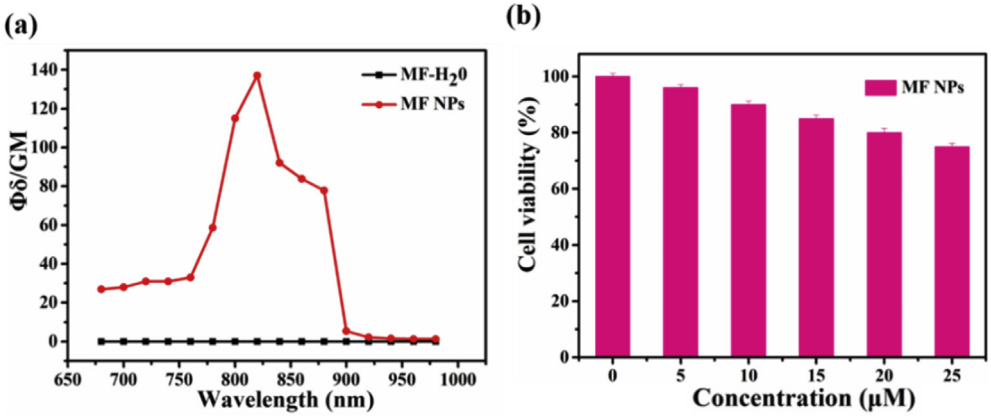

Fig. 5. (a) Effective two-photon absorption cross sections of **MF-H_2O** and **MF NPs** in different excitation wavelengths with identical energy of 500 mW. (b) Cytotoxicity data results of **MF NPs** at different concentrations for 24 h.

by DLS and SEM measurements. It is worth noting that the AIE-active **MF NPs** showed enhanced emission intensity (Fig. 3) and prolongedfluorescence time (Fig. 4). It is reasonable to expect that **MF NPs** would show good uptake efficiency by living cells and giving bright imaging results.

In addition, **MF NPs** exhibited considerable two-photon action cross section within the wavelength range from 680 nm to 900 nm (Fig. 5a), corroborating that it could serve as a judicious candidate for two-photon bioimaging withhigher spacial resolution and weaker specimen photodamage [30]. Fortunately, **MF NPs** exhibited low toxicity evaluating via MTT assay (Fig. 5b). The comprehensive merits of **MF NPs** motivated us to explore its two-photon biological imaging application.

Using HeLa cells as a model, cell-staining experiments using two-photon confocal microscopy (2PM) were carried out. The results showed that **MF NPs** (10 μM, 20 min) could readily enter HeLa

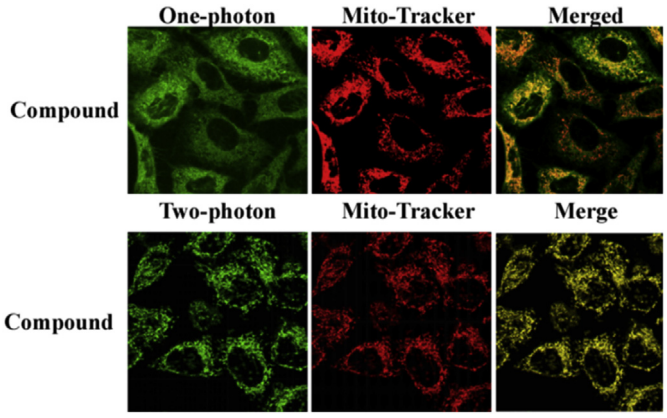

Fig. 6. One- and two-photon images of HeLa cells incubated with **MF NPs**, HeLa cells were incubated with **MF NPs** for 20 min, and then co-incubated with Mito tracker respectively for 20 min.

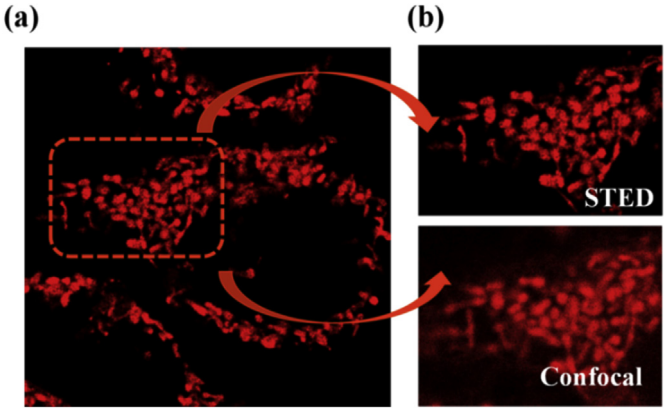

Fig. 7. STED micrographs of HeLa cells incubated with **MF NPs**. Scale bar: 100 nm. (a) Zoomed in STED micrograph from selected regions from (b) showing fibrillar mitochondria.

cells effectively and predominantly emission is apparently observed from mitochondria. To further confirm the cellular location of **MF NPs**, a commercial organelle marker Mito-tracker Red was introduced for co-localization experiments. As illuminated in Fig. 6, it strongly demonstrated that **MF NPs** could target the intracellular mitochondria *via* electrostatic interaction due to its cationic characteristic [31]. Additionally, stimulated emission depletion (STED) nanoscopy of **MF NPs** was performed owing to its longer excitation wavelength and good photo-stability. As shown in Fig. 7, the ultradetail of a single mitochondrion revealed fibrillar structures, highly correspondent to the distribution of **MF NPs** in mitochondria.

4. Conclusion

In this contribution, a D-π-A configuration molecular **MF** has been rationally fabricated to achieve two-photon activity for bioimaging. Thanks to the minor modification and cationic nature of **MF,** the obtained **MF** revealed AIE characteristics and could specific target mitochondria by using two-photon confocal microscopy and stimulated emission depletion nanoscopy methods.

Acknowledgements

This work was supported by a grant for the National Natural Science Foundation of China (21701160, 51672002, 51772002 and 21871003), Doctor Startup Fund (S020118002/026), Hefei National Laboratory for Physical Sciences at the Microscale (KF2019002), Natural science research project of universities in Anhui Province (KJ20191127).

Appendix A. Supplementary data

Supplementary data to this article can be found online at https://doi.org/10.1016/j.saa.2019.117571.

References

[1] M. Karbowski, R.J. Youle, Dynamics of mitochondrial morphology in healthy cells and during apoptosis, Cell Death Differ. 10 (2003) 870.
[2] I. Kim, S. Rodriguez-Enriquez, J.J. Lemasters, Selective degradation of mitochondria by mitophagy, Arch. Biochem. Biophys. 462 (2007) 245.
[3] N.J. Dolman, K.M. Chambers, B. Mandavilli, R.H. Batchelor, M.S. Janes, Tools and techniques to measure mitophagy using fluorescence microscopy, Autophagy 9 (2013) 1653.
[4] Y. Liu, J. Zhou, L. Wang, X. Hu, X. Liu, M. Liu, Z. Cao, D. Shangguan, W. Tan, A cyanine dye to probe mitophagy: simultaneous detection of mitochondria and autolysosomes in live cells, J. Am. Chem. Soc. 138 (2016) 12368.
[5] Y. Liu, L. Teng, L. Chen, H. Ma, H.-W. Liu, X.-B. Zhang, Engineering of a near-infrared fluorescent probe for real-time simultaneous visualization of intracellular hypoxia and induced mitophagy, Chem. Sci. 9 (2018) 5347.
[6] Z. Gao, Y. Li, F. Wang, T. Huang, K. Fan, Y. Zhang, J. Zhong, Q. Cao, T. Chao, J. Jia, S. Yang, L. Zhang, Y. Xiao, J.-Y. Zhou, X.-H. Feng, J. Jin, Mitochondrial dynamics controls anti-tumour innate immunity by regulating CHIP-IRF1 axis stability, Nat. Commun. 8 (2017) 1805.
[7] S. Zhang, T.-H. Chen, H.-M. Lee, J. Bi, A. Ghosh, M. Fang, Z. Qian, F. Xie, J. Ainsley, C. Christov, F.-T. Luo, F. Zhao, H. Liu, Luminescent probes for sensitive detection of pH changes in live cells through two near-infrared luminescence channels, ACS Sens. 2 (2017) 924.
[8] H. Ma, M. Yang, C. Zhang, Y. Ma, Y. Qin, Z. Lei, L. Chang, L. Lei, T. Wang, Y. Yang, Aggregation-induced emission (AIE)-active fluorescent probes with multiple binding sites toward ATP sensing and live cell imaging, J. Mater. Chem. B. 5 (2017) 8525.
[9] H. Ma, Y. Qin, Z. Yang, M. Yang, Y. Ma, P. Yin, Y. Yang, T. Wang, Z. Lei, X. Yao, Positively charged hyperbranched polymers with tunable fluorescence and cell imaging application, ACS Appl. Mater. Interfaces 10 (2018) 20064.
[10] S.H. Alamudi, D. Su, K.J. Lee, J.Y. Lee, J.L. Belmonte-Vázquez, H.-S. Park, E. Peña-Cabrera, Y.-T. Chang, A palette of background-free tame fluorescent probes for intracellular multi-color labelling in live cells, Chem. Sci. 9 (2018) 2376.
[11] F. Hu, Y. Yuan, W. Wu, D. Mao, B. Liu, Dual-responsive metabolic precursor and light-up AIEgen for cancer cell bio-orthogonal labeling and precise ablation, Anal. Chem. 90 (2018) 6718.
[12] A. Jiménez-Sánchez, E.K. Lei, S.O. Kelley, A multifunctional chemical probe for the measurement of local micropolarity and microviscosity in mitochondria, Angew. Chem. Int. Ed. 57 (2018) 8891.
[13] G. Lukinavičius, G.Y. Mitronova, S. Schnorrenberg, A.N. Butkevich, H. Barthel, V.N. Belov, S.W. Hell, Fluorescent dyes and probes for super-resolution microscopy of microtubules and tracheoles in living cells and tissues, Chem. Sci. 9 (2018) 3324.
[14] L. Sansalone, S. Tang, J. Garcia-Amorós, Y. Zhang, S. Nonell, J.D. Baker, B. Captain, F.M. Raymo, A photoactivatable far-red/near-infrared BODIPY to monitor cellular dynamics in vivo, ACS Sens. 3 (2018) 1347.
[15] Y. Zhang, S. Xia, M. Fang, W. Mazi, Y. Zeng, T. Johnston, A. Pap, R.L. Luck, H. Liu, New near-infrared rhodamine dyes with large Stokes shifts for sensitive sensing of intracellular pH changes and fluctuations, Chem. Commun. 54 (2018) 7625.
[16] B. Dong, X. Kong, W. Lin, Reaction-based fluorescent probes for the imaging of nitroxyl (HNO) in biological systems, ACS Chem. Biol. 13 (2017) 1714.
[17] C. Zhu, L. Liu, Q. Yang, F. Lv, S. Wang, Water-soluble conjugated polymers for imaging, diagnosis, and therapy, Chem. Rev. 112 (2012) 4687.
[18] J. Zhou, H. Ma, Design principles of spectroscopic probes for biological applications, Chem. Sci. 7 (10) (2016) 6309.
[19] W. Xu, Z. Zeng, J.-H. Jiang, Y.-T. Chang, L. Yuan, Discerning the chemistry in individual organelles with small-molecule fluorescent probes, Angew. Chem. Int. Ed. 55 (2016) 13658.
[20] Z. Yang, A. Sharma, J. Qi, X. Peng, D.Y. Lee, R. Hu, D. Lin, J. Qu, J.S. Kim, Super-resolution fluorescent materials: an insight into design and bioimaging applications, Chem. Soc. Rev. 45 (2016) 4651.
[21] C.M. Ackerman, S. Lee, C.J. Chang, Analytical methods for imaging metals in biology: from transition metal metabolism to transition metal signaling, Anal. Chem. 89 (2017) 22.
[22] A. Haque, M.S.H. Faizi, J.A. Rather, M.S. Khan, Next generation NIR fluorophores for tumor imaging and fluorescence-guided surgery: a review, Bioorg. Med. Chem. 25 (2017) 2017.
[23] A.S. Klymchenko, Solvatochromic and fluorogenic dyes as environment-sensitive probes: design and biological applications, Acc. Chem. Res. 50 (2017) 366.
[24] D. Li, X. Tian, A. Wang, L. Guan, J. Zheng, F. Li, S. Li, H. Zhou, J. Wu, Y. Tian,

Nucleic acid-selective light-up fluorescent biosensors for ratiometric two-photon imaging of the viscosity of live cells and tissues, Chem. Sci. 7 (2016) 2257.
[25] G.S. He, L.-S. Tan, Q. Zheng, P.N. Prasad, Multiphoton absorbing materials: molecular designs, characterizations, and applications, Chem. Rev. 108 (2008) 1245.
[26] C. Zhang, Y. Zhao, D. Li, J. Liu, H. Han, D. He, Y. Tian, S. Li, J. Wu, Y. Tian, Aggregation-induced emission (AIE)-active moleculesbearing singlet oxygen generation activities: the tunable singlet−triplet energy gap matters, Chem. Commun. 55 (2019) 1450.
[27] R. Zhang, G. Niu, X. Li, L. Guo, H. Zhang, R. Yang, Y. Chen, X. Yu, B.Z. Tang, Reaction-free and MMP-independent fluorescent probes for long-term mitochondria visualization and tracking, Chem. Sci. 10 (2019) 1994.
[28] J. Xiong, K. Wang, Z. Yao, B. Zou, J. Xu, X.-H. Bu, Multi-stimuli-Responsive fluorescence switching from a pyridine-functionalized tetraphenylethene AIEgen, ACS Appl. Mater. Interfaces 10 (2018) 5819.
[29] J. Xiong, X. Li, C. Yuan, S. Semin, Z. Yao, J. Xu, T. Rasing, X.-H. Bu, Wavelength dependent nonlinear optical response of tetraphenylethene aggregation-induced emission luminogens, Mater. Chem. Front. 2 (2018) 2263.
[30] X. Tian, Y. Zhu, M. Zhang, L. Luo, J. Wu, H. Zhou, L. Guan, G. Battagliade, Y. Tian, Localization matters: a nuclear targeting two-photon absorption iridium complex in photodynamic therapy, Chem. Commun. 53 (2017) 3303.
[31] D. Liu, M. Zhang, W. Du, L. Hu, F. Li, X. Tian, A. Wang, Q. Zhang, Z. Zhang, J. Wu, Y. Tian, A series of Zn (II) terpyridine-based nitrate complexes as two-photon fluorescent probe for identifying apoptotic and living cells via subcellular immigration, Inorg. Chem. 57 (2018) 7676.